Improved Region-Scalable Fitting Model with Robust Initialization for Image Segmentation

Keyan Ding
School of Mechanical and Electric Engineering
Soochow University
Suzhou, China
kyding@stu.suda.edu.cn

Guirong Weng
School of Mechanical and Electric Engineering
Soochow University
Suzhou, China
wgr@suda.edu.cn

***Abstract*—It had been known the region-scalable fitting (RSF) model can handle images with intensity inhomogeneity effectively, but it depends on the position of the initial contour. In this paper, we present a scheme to improve the robustness of initialization in the original RSF model. In the process of curve evolution, we add a function to exchange the value of fitting inside and outside curve in the regions where the direction of curve evolution is opposite. In this way, the whole curve will evolve along the inner or outer boundary of object. Thus, the improved RSF model will not be trapped in local minima. The experimental results have proved the proposed scheme is robust to initialization. And compared to other improvements, our proposed scheme is simple and efficient.**

Keywords-active contour, image segmentation, intensity inhomogeneity, level set method, region-scalable fitting.

I. INTRODUCTION

Image segmentation is a fundamental problem in the field of image processing and computer vision. Over the past decades, many famous image segmentation methods have been presented, such as region grow, watershed algorithm and graph cut. Active contour model has been extensively applied to image segmentation since the introduction by Kass *et al*. [1]. Active contour model can achieve sub-pixel accuracy of object boundaries and provide smooth and closed contours as segmentation results. Existing active contour models can be roughly categorized into two basic classes: *edge-based* models [2]–[5] and *region-based* models [6]–[12]. Edge-based models utilize an edge indicator to attract the curve toward the desired boundaries. Region-based models usually use image statistics to find a partition of image domain. The CV model, proposed by Chan and Vese [8], is one of the most popular region-based models, but it cannot work well for the images with intensity inhomogeneity. Li *et al.* [10] proposed a region-scalable fitting (RSF) model (originally termed as local binary fitting (LBF) model [11]). The RSF model draws upon intensity information in spatially varying local regions depending on a scale parameter. With the information of local image intensities, it is able to deal with intensity inhomogeneity accurately and efficiently. However, if the initial contour is set inappropriately, the energy of RSF model will be stuck in local minima due to the fact that energy functional is non-convex [13]. That means an improper initial contour will lead to a wrong segmentation result.

Wang *et al.* [14] proposed a model based on local and global intensity fitting (LGIF) energy, which combines the advantages of the LBF model and the CV model. But for different images, it is difficult to choose a suitable parameter w, which controls the weight of local and global intensity fitting energy. He *et al.* [15] proposed a weighted RSF model using local entropy. It allows more flexible initialization compared to the original RSF model. But the computational cost increased much due to the introduction of local entropy, and the problem of arbitrary initialization has not been solved. Bhadauria *et al.* [16] used the results of fuzzy C-means clustering (FCM) clustering to initialize the contour of RSF model. Similarly, Gupta *et al.* [17] used the results of Gaussian kernel induced fuzzy C-means (GKFCM) clustering to initialize the RSF model. This kind of approach may cause a wrong segmentation because it is difficult to ensure that the every pre-segmentation results are desirable for different images.

In this paper, we present an improved RSF model with robust initialization. First, we analyze the reason why the RSF model is sensitive to initialization from the perspective of curve evolution. Then, we construct a function to exchange the value of fitting functions in the regions where the direction of curve evolution is opposite. By adding this exchange function to the process of curve evolution, the whole curve will evolve along the inner or outer boundary of object. Experiments shows that the proposed scheme can improve the robustness of initialization and meanwhile retain the advantages of original RSF model.

II. BACKGROUNDS

The basic idea of RSF model is to define a local intensity fitting energy by introducing a kernel function, that is

$$\begin{aligned}\varepsilon^{RSF}(C, f_1, f_2) = \lambda_1 \int_{\Omega} \Big(\int_{out(C)} K(x-y)\,|\,I(y) - f_1(x)\,|^2\, dy \Big) dx \\ + \lambda_2 \int_{\Omega} \Big(\int_{in(C)} K(x-y)\,|\,I(y) - f_2(x)\,|^2\, dy \Big) dx\end{aligned} \quad (1)$$

where, K is a Gaussian kernel with standard deviation σ. f_1

and f_2 are two smooth functions that approximate the local image intensities inside and outside the contour C, respectively.

The curve can be represented by the zero-level set of a Lipschitz function ϕ, which takes positive and negative values outside and inside the contour, respectively. The energy functional $\varepsilon^{\mathrm{RSF}}$ can be expressed as

$$\begin{aligned}\varepsilon^{RSF}(\phi, f_1, f_2) = \lambda_1 \int (\int K(x-y)\,|\,I(y)-f_1(x)\,|^2\, H(\phi)dy)dx \\ +\lambda_2 \int (\int K(x-y)\,|\,I(y)-f_2(x)\,|^2\, (1-H(\phi))dy)dx\end{aligned} \tag{2}$$

In practice, the Heaviside function $H(x)$ in the above energy functional is approximated by a smooth function $H_\varepsilon(x)$ defined by

$$H_\varepsilon(x) = \frac{1}{2}(1+\frac{2}{\pi}\arctan(\frac{x}{\varepsilon})) \tag{3}$$

The derivative of H_ε is

$$\delta_\varepsilon(x) = \frac{\varepsilon}{\pi(\varepsilon^2 + x^2)} \tag{4}$$

In order for stable evolution of level set function, a distance regularized term $P(\phi)$ in [13] is incorporated into (2). And the Euclidean length term $L(\phi)$ in [13] is used to smooth the curve. Therefore, the entire energy functional E^{RSF} can be expressed as

$$E^{RSF}(\phi, f_1, f_2) = \varepsilon^{RSF}(\phi, f_1, f_2) + \upsilon L(\phi) + \mu P(\phi) \tag{5}$$

Minimizing the above energy functional by standard gradient descent method, the following variational formulations can be obtained:

$$\frac{\partial \phi}{\partial t} = -\delta_\varepsilon(\phi)(\lambda_1 e_1 - \lambda_2 e_2) + \nu\delta_\varepsilon(\phi) div(\frac{\nabla\phi}{|\nabla\phi|}) + \mu(\nabla^2\phi - div(\frac{\nabla\phi}{|\nabla\phi|})) \tag{6}$$

where e_1 and e_2 are

$$\begin{cases} e_1(x) = \int_\Omega K_\sigma(y-x)\,|\,I(x)-f_1(y)\,|^2\, dy \\ e_2(x) = \int_\Omega K_\sigma(y-x)\,|\,I(x)-f_2(y)\,|^2\, dy \end{cases} \tag{7}$$

with

$$\begin{cases} f_1(x) = \dfrac{\int_\Omega K_\sigma(x-y)[H_\varepsilon(\phi(y))\cdot I(y)]dy}{\int_\Omega K_\sigma(x-y)H_\varepsilon(\phi(y)dy} \\ f_2(x) = \dfrac{\int_\Omega K_\sigma(x-y)[(1-H_\varepsilon(\phi(y))\cdot I(y)]dy}{\int_\Omega K_\sigma(x-y)[1-H_\varepsilon(\phi(x)]dy} \end{cases} \tag{8}$$

The standard deviation σ of the kernel plays an important role in the RSF model. It can be seen as a scale parameter that controls the region-scalability from small neighborhood to the whole image domain. This is why the RSF model can handle images with intensity inhomogeneity effectively.

III. THE PROPOSED SCHEME

A. *Analysis of the Drawback in the RSF Model*

We had known the RSF model can segment image with intensity inhomogeneity effectively, but tends to be stuck in local minima. In this section, we will analyze the reason why an inappropriate initial contour can result in a wrong segmentation from the perspective of curve evolution.

Take Fig. 1 for an example, it is a synthetic image with intensity inhomogeneity. The green line is initial contour, the red line is the contour after some iterations, and the blue arrows are the directions of curve evolution. Every row represents the process of curve evolution from the initial contour to the final contour. We can know from the first row of Fig. 1 that a partial curve located inside the object (denoted C_1) is evolving along the inner boundary, while another partial curve located outside the object (denoted C_2) is evolving along the outer boundary. Thus, the curve C_1 and C_2 cause a mutual repulsion due to the opposite direction of curve evolution. Finally, although the curve has covered all the boundaries of object, the excess curves that stuck in the middle of both background and foreground regions cannot be removed because the RSF energy has been minimized. Therefore, the segmentation result is wrong.

Ideally, the whole curve should be evolved along the inner boundary or the outer boundary, as shown in the second and last rows of Fig. 1, respectively. In these ways, the segmentation results are correct. Therefore, it is important to ensure that the whole curve evolves on the same side of boundary.

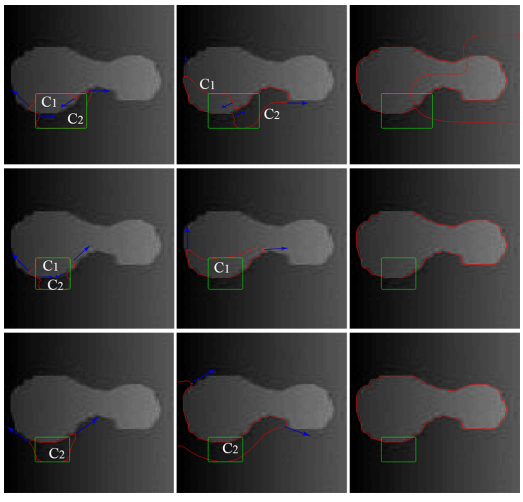

Figure 1. Analysis of curve evolution in the RSF model. The green line is initial contour, the red line is contour after some iterations, and the blue arrows are the directions of curve evolution. C_1 and C_2 denote the curve inside and outside the object, respectively. Every row represents the process of curve evolution from the initial contour (in the first column) to the final contour (in the third column).

B. *The Improved RSF model*

In this section, we will present an improved RSF model, which is robust to the initial contour. Note that f_1 and f_2 are the weighted averages of the image intensities in a local region outside and inside the curve, respectively. There is a key point that when the curve evolves along the inner boundary, the value of f_1 and f_2 are opposite to the value of f_1 and f_2 when the curve evolves along the outer boundary. It can be proved by seeing the values of f_1 and f_2 in the second and last rows of Fig. 1. The results are shown in Fig. 2.

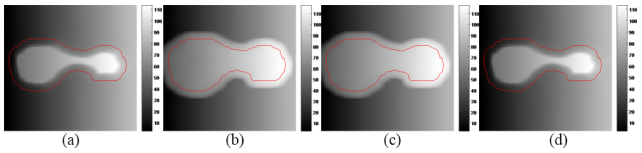

Figure 2. (a) and (b) are the values of f_1 and f_2 in the second row of Fig. 1, respectively. (c) and (d) are the values of f_1 and f_2 in the last row of Fig. 1 respectively.

Assuming that the whole curve evolves along the inner boundary is correct, we need to reverse the direction of the curve evolving along the outer boundary. Thus, the whole curve will evolve on the same side of boundary. Take the first row of Fig. 1 for an example, because Fig. 1 is an image with bright target and dark background, if the segmentation is correct, the value of f_1 should be less than f_2 near the boundaries, as shown in Fig. 3(a). In the process of curve evolution, if $f_1 > f_2$ on a certain region, it means the curve is evolving along the outer boundary, like the curve C_2 in Fig. 3(b). When the curve evolves along the outer boundary, the value of f_1 and f_2 are opposite to the value when the curve evolves along the inner boundary. Therefore, in the white regions where $f_1 > f_2$, we should exchange the value of f_1 and f_2 in each evolution, so that this partial curve will evolve along the inner boundary gradually. Finally, the whole curve will be evolved inside the boundary no matter where the initial contour located on, and a correct segmentation will be obtained.

On the contrary, if assuming that the whole curve evolves along the outer boundary is correct, we need to reverse the direction of the curve evolving along the inner boundary. That means exchanging the value of f_1 and f_2 in the black regions where $f_1 < f_2$. In this way, the whole curve will be evolved along the outer boundary, and a correct segmentation will also be obtained.

In summary, we construct an exchange function $\Psi(f_1, f_2, \Omega_x)$, which exchanges the value of f_1 and f_2 in each evolution at the region Ω_x. Note, Ω_x could be the region $\{x \mid f_1(x) > f_2(x)\}$, or the region $\{x \mid f_1(x) < f_2(x)\}$. It can be realized by using the mathematical *min* and *max* functions. Thus, when $\Omega_x = \{ x \mid f_1(x) > f_2(x)\}$,we use $min(f_1, f_2)$ and $max(f_1, f_2)$ to replace f_1 and f_2, respectively.

$$\begin{cases} f_1^*(x) = \min(f_1(x), f_2(x)) \\ f_2^*(x) = \max(f_1(x), f_2(x)) \end{cases} \tag{9}$$

When $\Omega_x = \{ x \mid f_1(x) < f_2(x)\}$,we use $max(f_1, f_2)$ and $min(f_1, f_2)$ to replace f_1 and f_2, respectively.

$$\begin{cases} f_1^*(x) = \max(f_1(x), f_2(x)) \\ f_2^*(x) = \min(f_1(x), f_2(x)) \end{cases} \tag{10}$$

The gradient descent flow of RSF model can be rewritten as:

$$\frac{\partial \phi}{\partial t} = -\delta_\varepsilon(\phi)(\lambda_1 e_1^* - \lambda_2 e_2^*) + \nu\delta_\varepsilon(\phi) div\left(\frac{\nabla\phi}{|\nabla\phi|}\right) + \mu\left(\nabla^2\phi - div\left(\frac{\nabla\phi}{|\nabla\phi|}\right)\right) \tag{11}$$

where e_1^* and e_2^* are

$$\begin{cases} e_1^*(x) = \int_\Omega K_\sigma(y-x) \mid I(x) - f_1^*(y) \mid^2 dy \\ e_2^*(x) = \int_\Omega K_\sigma(y-x) \mid I(x) - f_2^*(y) \mid^2 dy \end{cases} \tag{12}$$

Note, the variables and parameters in the original RSF model are totally unchanged except the fitting functions f_1 and f_2. In this way, the whole curve will evolve along the inner or outer boundary, and a correct segmentation result can be obtained. Therefore, the proposed scheme overcomes the shortcoming of RSF model that depends on the position of the initial contour just by a simple and efficient way.

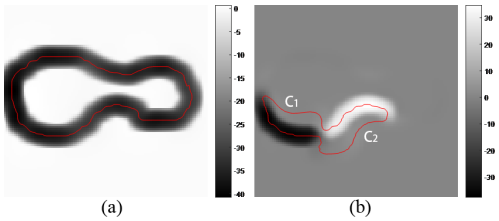

Figure 3. (a) The value of (f_1-f_2) corresponding to the second row of Fig. 1. (b) The value of (f_1-f_2) corresponding to the first row of Fig. 1.

IV. Experimental Results

In this section, the improved RSF model will be tested with synthetic and real images. Its implementation is consistent with the original RSF model. The initial level set function is initialized as a binary step function which takes a negative constant value $-c_0$ inside zero level set and a positive constant value c_0 outside. Unless otherwise specified, we use the following parameters in the improved model: c_0=2, σ=3, μ=1, υ=0.002×255^2, λ_1=λ_2=1 and time step Δt=0.1. The improved model is implemented in Matlab R2014a on a 2.6-GHz Inter(R) Core(TM) i5 personal computer.

First, we compare the improved RSF model with the original RSF models for the initial contour in the first rows of Fig. 1. From Fig. 4, we can know the curve that originally evolved on the outside of boundary have been evolved toward the inside of boundary. Thus, correct segmentation result is obtained.

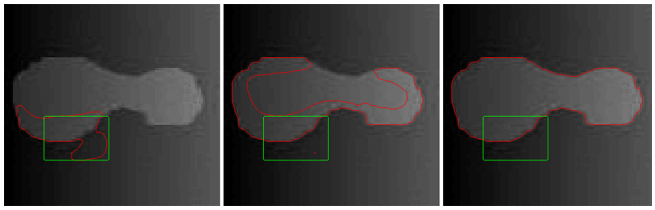

Figure 4. The process of curve evolution in the improved RSF model with the initial contour in the first rows of Fig. 1.

Fig. 5 shows the segmentation results of improved RSF model for four medical images. Where, the weight of length term ν are 0.005×255^2, 0.001×255^2, 0.001×255^2 and 0.002×255^2, respectively. These images have typical intensity inhomogeneity, weak edges or low contrast. Fig. 2 has demonstrated that the proposed model can obtain the satisfactory segmentation results for these images.

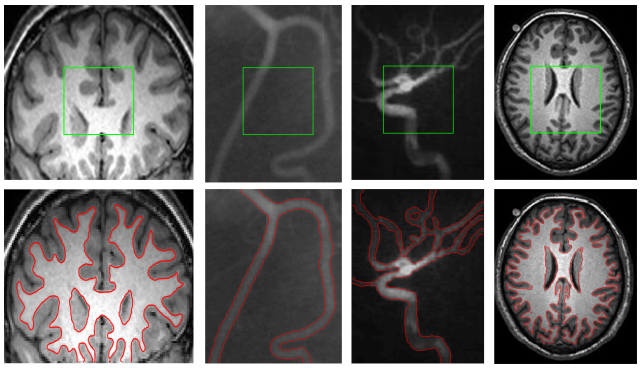

Figure 5. The segmentation results of some medical images in the improved RSF model. The initial contours and the final contours are plotted as the green lines and red lines, respectively.

Next, we choose a synthetic image with noise, a real image of leaf texture, and a complicated cerebral angiography image to test the robustness of initialization in the improved RSF model, as shown in Fig. 6 to Fig. 8, respectively. The segmentation results of the original RSF model and the improved RSF model are shown in upper row and lower row, respectively. In Fig. 5 and Fig. 6, only the first case of initial contour is segmented correctly in the original RSF model. But in the improved RSF model, each case of initial contour obtains a desirable result. In Fig. 7, the original RSF model cannot get a correct segmentation result due to this image is too complicated. In our improved RSF model, it is easy to segment correctly.

Table 1 shows the iteration numbers and segmentation time of the original RSF model [10], the weighted RSF model [15], the normalized RSF model [18], and the proposed improved RSF model for Fig. 6, Fig. 7 and Fig. 8. According to the experimental data in Table 1, we can know that the segmentation time of proposed model has hardly increased compared to original RSF model, and more efficient than weighted RSF model and normalized-based RSF model.

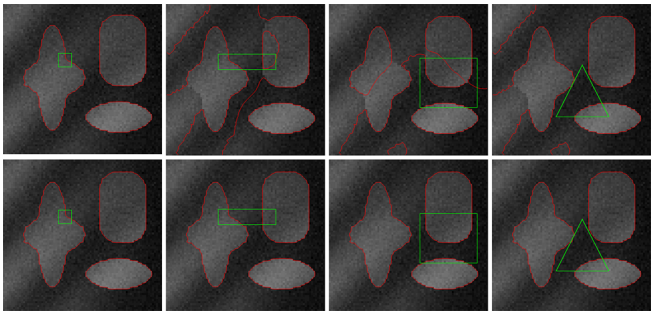

Figure 6. Applications of both RSF models to a synthetic image with noise (79×75 pixels).

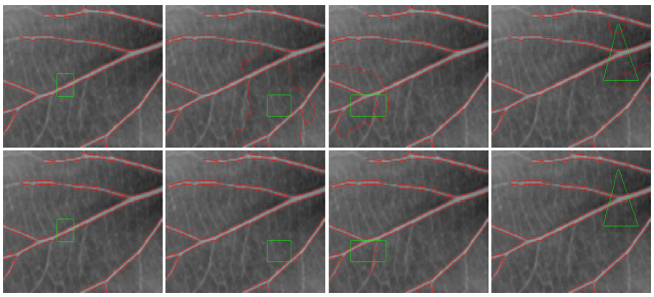

Figure 7. Applications of both RSF models to a real image of leaf texture (134×150 pixels).

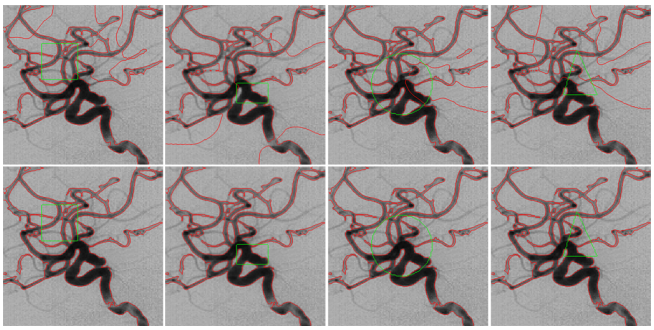

Figure 8. Applications of both RSF models to a cerebral angiography image (237×237 pixels).

TABLE I. COMPARISONS ON SEGMENTATION EFFICIENCY AMONG THE ORIGINAL, WEIGHTED, NORMALIZED, AND PROPOSED RSF MODEL FOR FIG. 6, FIG. 7 AND FIG. 8.

		Original	Weighted	Normalized	Proposed
Fig. 6	Iteration numbers	130	120	180	120
	Time (s)	1.145	1.482	2.248	1.112
Fig. 7	Iteration numbers	210	200	330	220
	Time (s)	2.149	2.781	3.699	2.209
Fig. 8	Iteration numbers	200	250	250	200
	Time (s)	3.050	3.800	4.451	3.105

V. CONCLUSION

In this paper, we have presented a scheme to improve the robustness of initialization in the original RSF model. By adding an exchange function into the process of curve evolution, the whole curve will evolve along the inner boundary or outer boundary of objects. Therefore, the improved RSF model is robust to the choice of initial contour. And compared to other improvements, our proposed scheme is simple and efficient. In addition, the proposed scheme can be applied to other models based on local intensity fitting energy.

REFERENCES

[1] M. Kass, A. Witkin, and D. Terzopoulos, "Snakes: Active contour models," Int. J. Comput. Vis., vol. 1, pp. 321–331, 1988.

[2] V. Caselles, R. Kimmel, and G. Sapiro, "Geodesic active contours," Int. J. Comput. Vis., vol. 22, no. 1, pp. 61–79, 1997.

[3] N. Paragios and R. Deriche, "Geodesic active contours and level sets for the detection and tracking of moving objects", IEEE Trans. Pattern Anal. Mach. Intell. vol. 22, no. 3, pp. 266–280, Mar. 2000.

[4] Y. Wang, L. Liu, H. Zhang, Z. Cao, and S. Lu, "Image segmentation using active contours with normally biased GVF external force", Signal Process. Lett., vol. 17, no. 10, pp. 875–878, 2010.

[5] C. Li, C. Xu, C. Gui, and M.D. Fox, "Distance regularized level set evolution and its application to image segmentation", IEEE Trans. Image Process., vol. 19, no. 12, pp. 3243–3254, 2010.

[6] D. Mumford and J. Shah, "Optimal approximation by piecewise smooth function and associated variational problems", Commun. Pure. Appl. Math., vol. 42, pp. 577–685, 1989.

[7] R. Ronfard, "Region-based strategies for active contour models", Int J. Comput. Vis., vol. 13, no. 2, pp. 229–251, 1994.

[8] T. Chan and L. Vese, "Active contours without edges", IEEE Trans. Image Process., vol. 10, no. 2, pp. 266–277, 2001.

[9] L. Vese and T. Chan, "A multiphase level set framework for image segmentation using the Mumford–Shah model", Int. J. Comput. Vis., vol. 50, no. 3, pp. 271–293, Dec. 2002

[10] C. Li, C. Kao, J. Gore, and Z. Ding, "Minimization of region-scalable fitting energy for image segmentation", IEEE Trans. Image Process., vol. 17, no. 10, pp. 1940–1949, Oct. 2008.

[11] C. Li, C. Kao, J. Gore, and Z. Ding, "Implicit active contours driven by local binary fitting energy", in IEEE Conf. Computer Vision and Pattern Recognition, Washington, DC, USA, 2007, pp. 1–7.

[12] K. Ding and G. Weng, "Robust active contours for fast image segmentation", Electron. Lett., vol. 52, no. 20, pp. 1687-1688, 2016.

[13] C. Dongye, Y. Zheng, and D. Jiang, "A Fast Global Minimization of Region-Scalable Fitting Model for Medical Image Segmentation", vol. 9, no. 2, pp. 280-286, Feb. 2014.

[14] L. Wang, C. Li, Q. Sun, D. Xia, and C. Kao, "Active contours driven by local and global intensity fitting energy with application to brain MR image segmentation", Comput. Med. Imag. Grap., vol. 33, pp. 520–531, 2009.

[15] C. He, Y. Wang, and Q. Chen, "Active contours driven by weighted region-scalable fitting energy based on local entropy", Signal Process., vol. 92, no. 2, pp. 587-600, 2012.

[16] H. Bhadauria and M. Dewal, "Intracranial hemorrhage detection using spatial fuzzy c-mean and region-based active contour on brain CT imaging", Signal Image Video P., vol. 8, no. 2, pp. 357-364, 2014.

[17] D. Gupta, R.S. Anand, and B. Tyagi, "A hybrid segmentation method based on Gaussian kernel fuzzy clustering and region based active contour model for ultrasound medical images", Biomed. Signal Proces., vol. 16, pp. 98–112, 2015.

[18] Y. Peng, F. Liu, and S, Liu, "Active contours driven by normalized local image fitting energy", Concurrency Computat.: Pract. Exper., vol. 26, pp. 1200–1214, 2014.

AUTHORS' BACKGROUND

Your Name	Title*	Research Field	Personal website
Keyan Ding	Master Student	Image Processing, Signal Processing, and Pattern Recognition	
Guirong Weng	Full Professor	Image Processing, Signal Processing, and Pattern Recognition	

*This form helps us to understand your paper better, the form itself will not be published.

*Title can be chosen from: master student, Phd candidate, assistant professor, lecture, senior lecture, associate professor, full professor